Oxygen Evolution Reaction

Deutsche Ausgabe: DOI: 10.1002/ange.201509643
Internationale Ausgabe: DOI: 10.1002/anie.201509643

A Mononuclear Co^{II} Coordination Complex Locked in a Confined Space and Acting as an Electrochemical Water-Oxidation Catalyst: A "Ship-in-a-Bottle" Approach

*Paulami Manna, Joyashish Debgupta, Suranjana Bose, and Samar K. Das**

Abstract: *Preparing efficient and robust water oxidation catalyst (WOC) with inexpensive materials remains a crucial challenge in artificial photosynthesis and for renewable energy. Existing heterogeneous WOCs are mostly metal oxides/hydroxides immobilized on solid supports. Herein we report a newly synthesized and structurally characterized metal–organic hybrid compound [{$Co_3(\mu_3$-OH)$(BTB)_2(dpe)_2$} {$Co(H_2O)_4(DMF)_2$}$_{0.5}$]$_n$·$n H_2O$ (**Co-WOC-1**) as an effective and stable water-oxidation electrocatalyst in an alkaline medium. In the crystal structure of **Co-WOC-1**, a mononuclear Co^{II} complex $\{Co(H_2O)_4(DMF)_2\}^{2+}$ is encapsulated in the void space of a 3D framework structure and this translationally rigid complex cation is responsible for a remarkable electrocatalytic WO activity, with a catalytic turnover frequency (TOF) of 0.05 s^{-1} at an overpotential of 390 mV (vs. NHE) in 0.1*M *KOH along with prolonged stability. This host–guest system can be described as a "ship-in-a-bottle", and is a new class of heterogeneous WOC.*

Water oxidation catalysis is one of the most contemporary research areas, not only because of its fundamental importance (high kinetic barrier and higher oxidation potential with the involvement of four electrons: $2H_2O \rightarrow O_2 + 4H^+ + 4e^-$) but also because of the increasing demand for renewable and sustainable energy utilization (reduction of protons to hydrogen).[1–4] A large number of research groups, worldwide, have been working to mimic water oxidation in natural photosynthesis by obtaining a catalyst which can function with low overpotential under ambient conditions in multiple cycles without any loss of catalytic activity.[5–8] Such natural reactions occur in aqueous solutions and are facilitated by homogeneous catalysts (e.g., metalloenzymes). Relevant homogeneous catalysis for chemical[9] as well as photochemical[10] water oxidations have been attempted to demonstrate the potential of homogeneous catalysts; however in many cases, the conditions under which these catalysts are used, make them susceptible to irreversible transformations to heterogeneous metal oxide particles.[11] Indeed, it is now an important subject to distinguish between true homogeneous catalysis by metal coordination complexes and heterogeneous catalysis by metal or metal oxide particles.[12] Artero and Fontecave, in a recent Review, have demonstrated that in a number of cases, the true catalytic species is heterogeneous in nature, arising from the transformation of the initial molecular species under the reaction conditions.[13] For example, some cobalt compounds that were initially thought to be water oxidation catalysts (WOCs), were later confirmed by Finke and Stracke as decomposition products of the actual catalyst.[11] In another instance, Nocera group shows that a small amount of Co^{II} impurity can be responsible for electrocatalytic water oxidation activity in an otherwise inactive $\{Co_4O_4\}$ cubane type molecular complex.[14] Thus, even though, cobalt oxygen-evolution catalysts (Co-OECs) have received immense attention in recent years because of their extensive use in photocatalytic as well electrocatalytic water-oxidation reactions,[15–19] great care has to be taken to identify the actual WOC species (whether the used molecular complex or its decomposed product!), especially in the case of homogeneous catalysis.[9,10] Hence, designing and synthesizing a well-defined and stable heterogeneous WOC is a daunting challenge in the area of catalytic water oxidation. A heterogeneous electrocatalyst, for example, prepared by depositing/coating a catalytically active material on the electrode surface, is of particular interest because it offers an extra stability and it can directly be implemented into devices.[6,20,21] Nocera and co-workers, the pioneering group in this area, have demonstrated the formation of water oxidation electrocatalysts by anodic electrodeposition of metal oxides from aqueous solutions of cobalt, nickel, and manganese salts.[20,22–27]

Metal–organic frameworks (MOFs) having well-defined void spaces/cages are generally good hosts,[28–31] capable of encapsulating an active guest.[32] In the last few years, we have been engaged in understanding the mechanistic aspects for the formation of metal–organic frameworks (MOFs) using flexible organic linkers.[33–36] In this journey, we have recently synthesized and structurally characterized a Co-based MOF [{$Co_3(\mu_3$-OH)$(BTB)_2(dpe)_2$}{$Co(H_2O)_4(DMF)_2$}$_{0.5}$]$_n$·$n H_2O$ (**Co-WOC-1**) [H_3BTB = 1,3,5-benzenetribenzoic acid; dpe = 1,2-di(4-pyridyl)ethylene, see Figure 1b,c], the crystal structure of which shows a mononuclear cobalt(II) complex cation $[Co^{II}(H_2O)_4(DMF)_2]^{2+}$, entrapped inside the void space of the framework (the mononuclear complex is not coordinated/attached to the host framework) in compound **Co-WOC-1**.

Although few recent reports illustrate the catalytic water oxidation potential of MOFs, combined with molecular catalysts, in developing heterogeneous WOCs,[32,37,38] a well-

[*] P. Manna, Dr. J. Debgupta, Dr. S. Bose, Prof. S. K. Das
School of Chemistry
University of Hyderabad
P.O. Central University, Hyderabad 500046 (India)
E-mail: skdas@uohyd.ac.in
samar439@gmail.com

Supporting information for this article (details of synthesis of compounds, electrode preparation, characterization techniques including single crystal structure determination and electrochemical measurements) is available on the WWW under http://dx.doi.org/10.1002/anie.201509643.

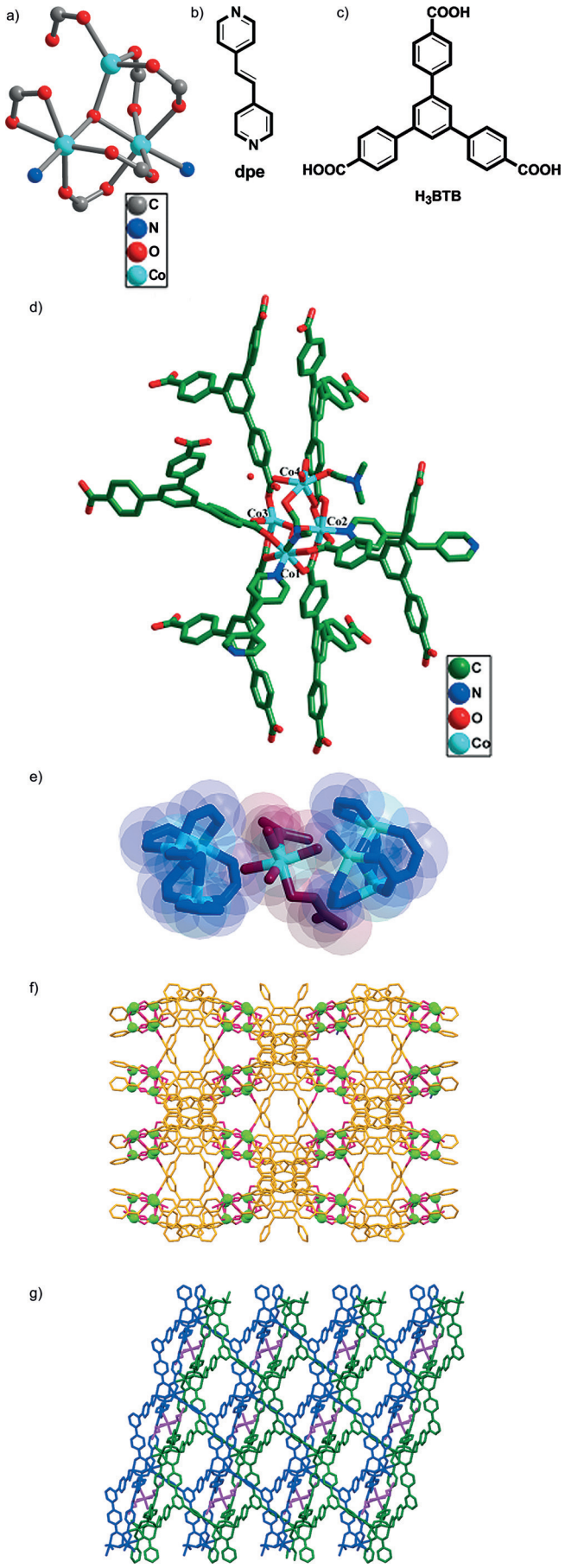

defined and structurally characterized cobalt-based MOF acting as WOC is rarely known.[39,40] Recently, water oxidation catalytic activity has been demonstrated using a Prussian blue-type cobalt hexacyanoferrate (CoHCF) coordination-polymer modified electrode that has been obtained by plating a FTO electrode with metallic cobalt followed by applying a positive potential (0.5 V vs. normal hydrogen electrode (NHE)) in a solution containing hexacyanoferrate(III).[39] Another report by Wang et al. demonstrates a cobalt-containing zeolite-type imidazolate framework (Co-ZIF-9, where cobalt is the part of the framework) to electrocatalyze the oxygen evolution reaction (OER).[40] Lin and co-workers have reported two highly porous and stable Zr-carboxylate MOFs, that act as efficient catalysts for Ce^{4+}-driven water oxidation.[38] The same group incorporated three iridium-based WOCs into the $Zr_6O_4(OH)_4(bpdc)_6$ (UiO-67, bpdc = *para*-biphenyldicarboxylate) framework resulting in the formation of three new MOFs, that also exhibit catalytic water oxidation.[37] The work done by Nepal and Das demonstrating water oxidation, catalyzed by a metal–organic cage isolated manganese dimer,[32] encouraged us to investigate whether the encapsulated Co^{II} species in the confined space of MOF (**Co-WOC-1**) can act as an efficient WOC. Herein we report a stable electrocatalyst, obtained by coating the compound **Co-WOC-1** onto an electrode surface, for sustained water oxidation.

Blue-violet block-shaped crystals of **Co-WOC-1** were harvested by heating a reaction mixture of $CoCl_2{\cdot}6H_2O$ (6.0 mg, 0.25 mmol), H_3BTB (11.0 mg, 0.25 mmol), and dpe (4.5 mg, 0.25 mmol) in 10 mL water/DMF (H_2O:DMF = 6:4) at 120 °C under solvothermal conditions. Single-crystal analysis revealed that **Co-WOC-1** crystallizes in the monoclinic space group *C*2/*c* (see Sections S1 and S2 in the Supporting Information for detailed synthetic procedure and characterization techniques). A unique $\{Co_3(\mu_3\text{-}OH)(COO)_6\}^{1-}$ trinuclear cluster was formed in situ which acts as a building block in construction of a 3D interpenetrated framework. The trimeric $\{Co_3(\mu_3\text{-}OH)(COO)_6\}^{1-}$ unit (Figure 1 a) is formed by the three Co^{II} metal ions, in which two have an octahedral $\{CoO_5N\}$ coordination and the other is a tetrahedral $\{CoO_4\}$ coordination sphere. The three Co^{II} centers, situated at the vertices of a scalene triangle (Co···Co distances are in range of 3.196–3.542 Å) are connected by a bridging OH group (μ_3-OH), situated roughly at the center of the triangle (Figure 1 a). Four carboxylate groups, involved in cluster composition, bridge the Co^{II} centers in bidentate coordination mode resulting in the formation of a low symmetry cluster. The connectivity of the $\{Co_3\}$ clusters along the skeletons of the

Figure 1. a) Basic trinuclear $\{Co_3(\mu_3\text{-}OH)(COO)_6\}^{-}$ unit. b) Linker dpe, c) Linker H_3BTB, d) Molecular diagram of the **Co-WOC-1** (hydrogen atoms are omitted for clarity). e) The space-filling plot of the encapsulated $\{Co(H_2O)_4(DMF)_2\}^{2+}$ coordination complex (in the middle), clutched by two different $\{Co_3\}$ units. f) Anionic framework of **Co-WOC-1** along the crystallographic *c* axis (the encapsulated complex cation $\{Co(H_2O)_4(DMF)_2\}^{2+}$ has been omitted) Co green, O purple, C yellow. g) Interpenetrated framework (frameworks shown in blue and green) along the crystallographic *b* axis with sterically crowded $\{Co(H_2O)_4(DMF)_2\}$ complex (purple).[44]

dpe linker (Figure 1 b) and BTB^{3-} linker (Figure 1 c) results in the construction of a 3D framework, and in the crystal structure, two such frameworks are interpenetrated to each other (Figures 1 f,g; see Section S4 in Supporting Information for the topological discussion).

An exceptional structural feature of compound **Co-WOC-1** is the encapsulation of a mononuclear Co^{II} complex cation, $\{Co(H_2O)_4(DMF)_2\}^{2+}$ (Figure 1 e) in the void space of 3D framework (Figure 1 f) resulting in a host-guest supramolecular system (Figure 1 g). The negative charges of two trinuclear clusters, $2\{Co_3(\mu_3\text{-}OH)(COO)_6\}^{1-}$ are counterbalanced by one cobalt complex cation $\{Co(H_2O)_4(DMF)_2\}^{2+}$, consistent with molecular formula: $[\{Co_3(\mu_3\text{-}OH)(BTB)_2(dpe)_2\}\text{-}\{Co(H_2O)_4(DMF)_2\}_{0.5}]_n\cdot n\,H_2O$ (**Co-WOC-1**). The position of the encapsulated $\{Co(H_2O)_4(DMF)_2\}^{2+}$ complex cation is located near to the anionic $\{Co_3(\mu_3\text{-}OH)(COO)_6\}^{1-}$ building block as a result of electrostatic columbic forces between both the associated ions. In the crystal, the mononuclear complex cation (guest) is trapped in a sterically crowded position between two interpenetrated frameworks (see Figures 1 e,g), so that it cannot come out of the overall framework, which results in a situation, equivalent to "ship-in-a-bottle". This crowding hinders the translation of the guest complex cation in any direction.

To explore the catalytic activity of **Co-WOC-1** towards water oxidation, we have performed extensive electrochemical studies. One clear quasi-reversible couple (A1/C1) is apparent in the cyclic voltammogram (Figure 2 a) of **Co-WOC-1** in 0.1 M KOH. This couple ($E_{A1} = 0.41$ V, $E_{C1} = 0.32$ V and $E_{1/2} = 0.37$ V vs. NHE with $\Delta E_{A1/C1} = 0.09$ V) can be assigned to the oxidation of Co^{II} to Co^{III}. Interestingly, the peak positions shift towards more negative potential when the pH of the electrolyte solution is lowered from pH 13 (0.1 M KOH) to pH 8 (phosphate buffer) (Figure S9a). This suggests that this quasi-reversible couple is due to the well-known proton-coupled electron transfer (PCET), as has been observed by Meyer and co-workers.[41] The plot of peak potential versus pH produces a straight line with a slope of 121 mV/pH (Figure S9b). This value of the slope suggests again the proton-coupled electron transfer ($1e^-/2H^+$) as has been observed by Meyer and co-workers.[42] A second but little broader peak (A2, Figure 2 a) ($E_{A2} = 0.71$ V vs. NHE), that appears prior to oxygen evolution, can be ascribed to the formation of higher valent Co^{IV} species (most probably Co^{IV}=O) which is the active intermediate for water oxidation. To access the kinetic aspect of the **Co-WOC-1** catalyst, Tafel plots, which relate overpotential (η) and catalytic current density, have been constructed by galvanostatic polarization technique at steady state. The Tafel plot at pH 13 (0.1 M KOH) shows linear behavior for a wide potential range with a Tafel slope of 128 mV/decade (Figure 2 b), establishing **Co-WOC-1** as an efficient catalyst for water oxidation.

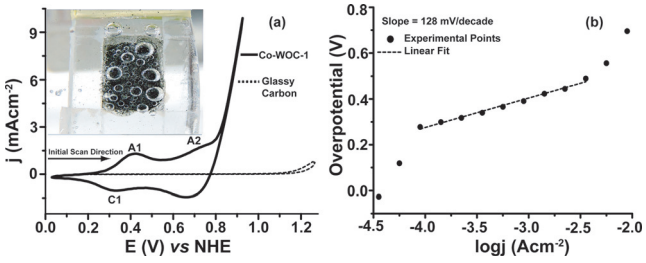

Figure 2. a) Cyclic voltammograms of **Co-WOC-1** (solid line) coated on a glassy carbon electrode (3 mm diameter) in 0.1 M KOH (pH 13) at scan rates of 100 $mV\,s^{-1}$ and the profile for glassy carbon electrode (dotted line). See text for assignments. Inset: Photograph of an FTO electrode coated with **Co-WOC-1** during electrolysis showing O_2 bubbles. b) Galvanostatic iR corrected Tafel plot of **Co-WOC-1** at pH 13. Tafel plots at pH 10 and 11 are in Figure S10.

An overpotential (η) of 390 mV has been calculated for this catalyst at a current density of 1 $mA\,cm^{-2}$ (for calculation, see Supporting Information). The value of this overpotential is in good agreement with other well established Co-based WOCs.[39] The overpotential has been found to increase with decrease in pH value (Figure S10). This suggests that the present catalyst (**Co-WOC-1**) performs best in pH 13. The reason for better performance of the present catalyst at higher pH towards electrocatalytic water oxidation can be understood from the viewpoint of stability of **Co-WOC-1** at different pH values during electrochemical experiments. In the present study, the negative charge of the host framework $\{Co_3(\mu_3\text{-}OH)(BTB)_2(dpe)_2\}_2^{1-}$ (which is inactive towards water oxidation) is counter balanced by the mononuclear complex cation $\{Co(H_2O)_4(DMF)_2\}_{0.5}^{1+}$ (which is the active species towards water oxidation). The water oxidation demands the oxidation of mononuclear cobalt complex, thereby the increase of positive charge of the guest. In this situation, the framework host would be unstable unless the system acquires negative charge corresponding to the increase in positive charge by oxidation of the guest. Thus water oxidation at higher pH is favored, because coordination of OH^- (from an aqueous KOH medium at pH 13) to mononuclear cobalt ion compensates the extra positive charge of the overall host–guest system. It should be noted that the title compound $[\{Co_3(\mu_3\text{-}OH)(BTB)_2(dpe)_2\}\{Co(H_2O)_4(DMF)_2\}_{0.5}]_n\cdot n\,H_2O$ is characterized with a protonated μ_3-OH group. Thus at pH 13 in an aqueous KOH medium, a deprotonation reaction is expected as follows [Eq. (1)]:

$$[\{Co_3(\mu_3\text{-}OH)(BTB)_2(dpe)_2\}\{Co(H_2O)_4(DMF)_2\}_{0.5}]_n\cdot n\,H_2O + KOH \rightarrow \text{(\textbf{Co-WOC-1})}$$
$$[K\{Co_3(\mu_3\text{-}O)(BTB)_2(dpe)_2\}\{Co(H_2O)_4(DMF)_2\}_{0.5}]_n\cdot n\,H_2O + H_2O \quad \text{(\textbf{KCo-WOC-1})} \qquad (1)$$

Thus after deprotonation reaction [Eq. (1)], inclusion of a K^+ ion per formula unit of the deprotonated product is anticipated. This deprotonation can be observed by a visual color change from a blue purple crystal (before dipping into an aqueous KOH solution) to a dark brown crystal (after dipping into an aqueous KOH solution for 10 min) and has been monitored by electronic absorption (diffuse reflectance) spectroscopy as shown in Figure 3. The presence of potassium in the deprotonated compound (**KCo-WOC-1**) has been confirmed by EDX and elemental mapping (Figure 3). On the

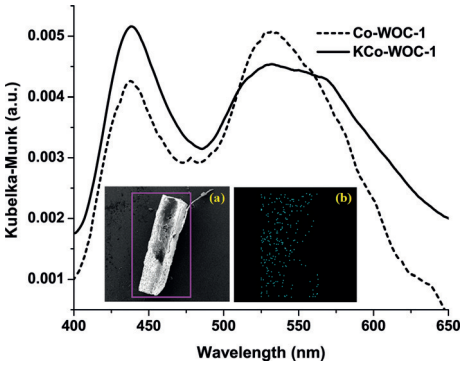

Figure 3. Diffuse reflectance spectra of **Co-WOC-1** and its deprotonated form (KCo-WOC-1); inset shows a) FESEM micrograph of KCo-WOC-1 and b) elemental mapping showing the distribution of K in KCo-WOC-1.

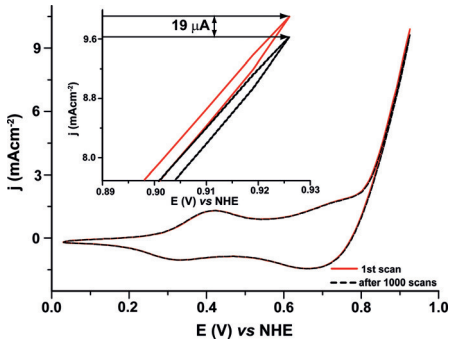

Figure 4. Stability test of **Co-WOC-1** during potential cycling (1000 scans), red solid (1st scan) and black dotted lines (1000th scan) cannot be distinguished because they appear almost in identical positions. Inset: cyclic voltammograms of **Co-WOC-1** in 0.1 M KOH before (red plot) and after (black plot) 1000 scans.

other hand, when electrocatalytic water oxidation is performed at a lower pH, the encapsulated Co^{II} complex does not show any oxidative response for the Co^{III}/Co^{II} couple, unlike that shown at a higher pH (10–13). This suggests that coordination of OH^- groups that facilitates the oxidation of encapsulated cobalt ion, is mandatory for this electrocatalytic water oxidation. This is why the present catalyst **Co-WOC-1** does not work at a low pH towards electrocatalytic water oxidation.

The catalyst shows a turnover frequency (TOF) of 0.05 s^{-1} at an overpotential of 390 mV at pH 13 (Section S9 in Supporting Information). The TOF value is the lower limit for the catalyst, based on the number of active Co atoms which take part in the catalysis, although the bulk of the material is electroactive. The number of active Co atoms participating in the water oxidation has been calculated from the peak current dependence of the oxidation peak for Co^{III}/Co^{II} couple (Figure S12) and is found to be 18.84 nmol cm^{-2} (Γ_o). Moreover, the quantitative measurement of the evolved oxygen gas (using gas chromatography, Figure S15) suggests that the oxygen-evolution process occurs with 96% Faradic efficiency and thereby confirms **Co-WOC-1** as an efficient catalyst for water oxidation. Additionally, **Co-WOC-1** has been found to be highly stable under harsh water-oxidation conditions (alkaline solution and high potential) and this aspect has an enormous impact as far as application in prolonged water electrolysis is concerned. The stability of **Co-WOC-1** under the electrolysis conditions has been probed by an accelerated durability test, in which 1000 cyclic voltammetric scans were performed from 0.05 to 0.9 V (vs. NHE) using this catalyst in pH 13 (Figure 4). No significant change in the catalytic current for WOC has been observed after 1000 scans, thereby suggesting that **Co-WOC-1** has an unprecedented stability during electrocatalytic water oxidation at a higher pH. However, very small drop in catalytic current (ca. 19 μA) can be attributed to mechanical loss of the sample from the glassy-carbon electrode surface during vigorous oxygen evolution at potential 0.9 V (vs. NHE).

The electrolyte solution, after 1000 scans, has been analyzed using the inductively coupled plasma (ICP) technique to confirm any possible leaching of cobalt from the catalyst. ICP result shows no detectable trace of cobalt in the electrolyte and hence rules out any possible destruction of the framework under the oxygen-evolution conditions. Moreover, EDX analysis of **KCo-WOC-1** before and after electrolysis (4.5 h) also supports the above outcome (Figure S6).

Even though **Co-WOC-1** is stabilized by a host–guest cooperative effect ("ship-in-a-bottle" manner) and the mononuclear cobalt complex cation $\{Co(H_2O)_4(DMF)_2\}^{2+}$ (guest) cannot be taken out from the host anion by ion exchange, we have claimed that only the guest complex cation is active towards water oxidation. The following experimental data provide explanations of why the guest complex cation (not the host framework) is responsible for this electrocatalytic water oxidation. When we perform the electrochemical experiments with **Co-WOC-1** at pH 4 (see Figure S11), we do not observe any redox response corresponding to Co^{III}/Co^{II} couple and thereby we do not observe water oxidation, in contrast to that we have seen at higher pH (see Figures 2a and 4). We have argued that the coordination of OH^- ion (at a higher pH) to the mononuclear cobalt center (guest) drives its oxidation and we see the quasi-reversible redox response corresponding to the Co^{III}/Co^{II} couple followed by water oxidation (Figures 2a and 4). This water oxidation is not possible at a lower pH (e.g., at pH 4, Figure S11) owing to the lack of OH^- ion coordination to the mononuclear cobalt center. The coordination of OH^- ion to a metal center, which has monodentate labile ligands, is expected. The coordination of framework cobalt centers is dominated by bidentate acetate-type chelate ligands (oxygen donors) and nitrogen donating dpe linker (Figure 1). Thus the preferred binding site of the OH^- ion during oxidation should be mononuclear (guest) cobalt complex $\{Co(H_2O)_4(DMF)_2\}^{2+}$, which has four labile water ligands and two disordered DMF ligands. During oxidation, if OH^- ion would have bound to a framework metal center, the system would have collapsed soon after one or two electrocatalytic cycle(s); instead we have achieved 1000 cycles without any loss of catalytic activity. Thus, if binding of the hydroxy ion is one of the prime events in this electrocatalytic water oxidation, the active species in this study has to be the guest mononuclear cobalt complex cation, $\{Co(H_2O)_4(DMF)_2\}^{2+}$. We also find some indirect support in favor of

guest species acting as an active site, when we experimentally determine the number of cobalt atoms participating in this electrocatalytic water oxidation. In a typical electrochemical experiment, the total number of active cobalt atoms is 1.33 nmol ($\Gamma_o = 18.84$ nmol cm^{-2}, see page S13 in Supporting Information for relevant calculations), which is much nearer to the value 7.15 nmol (calculated, when we consider only pore cobalt species) than the value of approximately 43 nmol (calculated, when we consider framework cobalt atoms). The deviation from the calculated value of 7.15 to the measured value of 1.33 can be correlated with the fact that only upper layer of the catalyst, deposited on the electrode surface, may be active towards oxidation.

In conclusion, electrochemical studies of compound **Co-WOC-1** have established it as an efficient electrocatalyst for water oxidation. Although, the catalyst performs best in an alkaline medium (pH 13) and the overpotential increases with decreasing pH, the stability and the turnover number of **Co-WOC-1** are remarkable as compared to those in the literature.[39,43] The host–guest system, **Co-WOC-1** is important from the fundamental point of view, because it provides a rare example of a structurally characterized MOF containing a compound that acts as an efficient electrocatalyst towards water oxidation. We have demonstrated that a mononuclear Co^{II} species, entrapped in a confined space of a framework structure, can act as an efficient electrocatalyst for water oxidation, which is so stable that it retains its stability even after 1000 cycles. This result opens up a new direction in the area of catalytic water oxidation in the sense that a Co^{II} species, encapsulated in a confined space of other known frameworks (for example, different zeolites, graphite type layered materials) might have potential to act as an efficient water-oxidation catalyst (WOC). We are presently working on this front to increase further efficiency of the heterogeneous WOCs.

Acknowledgements

We thank SERB, DST, Government of India (Project No. SB/S1/IC-34/2013) for financial support. P.M. thanks CSIR, New Delhi and J.D. and S.B. thank DSKPDF Scheme, UGC, New Delhi for fellowships. Mr. Ramsundar from CSIR-NCL, Pune is also acknowledged for helping in gas measurement studies (in GC). The National X-ray Diffractometer facility at University of Hyderabad by DST, Government of India, is gratefully acknowledged.

Keywords: electrocatalyst · metal–organic frameworks · cobalt complexes · oxygen evolution · water oxidation

How to cite: *Angew. Chem. Int. Ed.* **2016**, *55*, 2425–2430
Angew. Chem. **2016**, *128*, 2471–2476

[1] H. B. Gray, *Nat. Chem.* **2009**, *1*, 7.
[2] M. G. Walter, E. L. Warren, J. R. McKone, S. W. Boettcher, Q. Mi, E. A. Santori, N. S. Lewis, *Chem. Rev.* **2010**, *110*, 6446–6473.
[3] M. D. Kärkäs, O. Verho, E. V. Johnston, B. Åkermark, *Chem. Rev.* **2014**, *114*, 11863–12001.
[4] D. Z. Zee, T. Chantarojsiri, J. R. Long, C. J. Chang, *Acc. Chem. Res.* **2015**, *48*, 2027–2036.
[5] M. Ledney, P. K. Dutta, *J. Am. Chem. Soc.* **1995**, *117*, 7687–7695.
[6] D. G. Nocera, *Acc. Chem. Res.* **2012**, *45*, 767–776.
[7] J. J. Xing, W. Q. Fang, H. J. Zhao, H. G. Yang, *Chem. Asian J.* **2012**, *7*, 642–657.
[8] B. Limburg, E. Bouwman, S. Bonnet, *Coord. Chem. Rev.* **2012**, *256*, 1451–1467.
[9] Q. Yin, J. M. Tan, C. Besson, Y. V. Geletii, D. G. Musaev, A. E. Kuznetsov, Z. Luo, K. I. Hardcastle, C. L. Hill, *Science* **2010**, *328*, 342–345.
[10] Z. Huang, Z. Luo, Y. V. Geletii, J. W. Vickers, Q. Yin, D. Wu, Y. Hou, Y. Ding, J. Song, D. G. Musaev, C. L. Hill, T. J. Lian, *J. Am. Chem. Soc.* **2011**, *133*, 2068–2071.
[11] J. J. Stracke, R. G. Finke, *J. Am. Chem. Soc.* **2011**, *133*, 14872–14875.
[12] J. A. Widegren, R. G. Finke, *J. Mol. Catal. A* **2003**, *198*, 317–341.
[13] V. Artero, M. Fontecave, *Chem. Soc. Rev.* **2013**, *42*, 2338–2356.
[14] A. U. Ullman, Y. Liu, M. Huynh, D. K. Bediako, H. Wang, B. L. Anderson, D. C. Powers, J. J. Breen, H. D. Abruña, D. G. Nocera, *J. Am. Chem. Soc.* **2014**, *136*, 17681–17688.
[15] M. W. Kanan, Y. Surendranath, D. G. Nocera, *Chem. Soc. Rev.* **2009**, *38*, 109–114.
[16] J. B. Gerken, J. G. McAlpin, J. Y. C. Chen, M. L. Rigsby, W. H. Casey, R. D. Britt, S. S. Stahl, *J. Am. Chem. Soc.* **2011**, *133*, 14431–14442.
[17] J. Del Pilar-Albaladejo, P. K. Dutta, *ACS Catal.* **2014**, *4*, 9–15.
[18] M. Zhang, M. de Respinis, H. Frei, *Nat. Chem.* **2014**, *6*, 362–367.
[19] J. Del-Pilar, B. Wang, P. K. Dutta, *Microporous Mesoporous Mater.* **2015**, *217*, 125–132.
[20] M. W. Kanan, D. G. Nocera, *Science* **2008**, *321*, 1072–1075.
[21] Y. Gorlin, C.-J. Chung, J. D. Benck, D. Nordlund, L. Seitz, T.-C. Weng, D. Sokaras, B. M. Clemens, T. F. Jaramillo, *J. Am. Chem. Soc.* **2014**, *136*, 4920–4926.
[22] Y. Surendranath, M. Dinca, D. G. Nocera, *J. Am. Chem. Soc.* **2009**, *131*, 2615–2620.
[23] D. A. Lutterman, Y. Surendranath, D. G. Nocera, *J. Am. Chem. Soc.* **2009**, *131*, 3838–3839.
[24] M. Dinca, Y. Surendranath, D. G. Nocera, *Proc. Natl. Acad. Sci. USA* **2010**, *107*, 10337–10341.
[25] M. D. Symes, Y. Surendranath, D. A. Lutterman, D. G. Nocera, *J. Am. Chem. Soc.* **2011**, *133*, 5174–5177.
[26] D. K. Dogutan, Jr., R. McGuire, D. G. Nocera, *J. Am. Chem. Soc.* **2011**, *133*, 9178–9180.
[27] D. K. Bediako, B. Lassalle, Y. Surendranath, J. Yano, V. K. Yachandra, D. G. Nocera, *J. Am. Chem. Soc.* **2012**, *134*, 6801–6809.
[28] H. Furukawa, K. E. Cordova, M. O'Keeffe, O. Yaghi, *Science* **2013**, *341*, 1230444–1230456.
[29] M. Li, D. Li, M. O'Keeffe, O. M. Yaghi, *Chem. Rev.* **2014**, *114*, 343–1370.
[30] Y.-B. Zhang, H. Furukawa, N. Ko, W. Nie, H. J. Park, S. Okajima, K. E. Cordova, H. Deng, J. Kim, O. M. Yaghi, *J. Am. Chem. Soc.* **2015**, *137*, 2641–2650.
[31] J. Jiang, O. M. Yaghi, *Chem. Rev.* **2015**, *115*, 6966–6997.
[32] B. Nepal, S. Das, *Angew. Chem. Int. Ed.* **2013**, *52*, 7224–7227; *Angew. Chem.* **2013**, *125*, 7365–7368.
[33] P. Manna, B. K. Tripuramallu, S. K. Das, *Cryst. Growth Des.* **2012**, *12*, 4607–4623.
[34] P. Manna, B. K. Tripuramallu, S. K. Das, *Cryst. Growth Des.* **2014**, *14*, 278–289.
[35] P. Manna, S. K. Das, *Cryst. Growth Des.* **2015**, *15*, 1407–1421.
[36] P. Manna, B. K. Tripuramallu, S. Bommakanti, S. K. Das, *Dalton Trans.* **2015**, *44*, 2852–2864.
[37] C. Wang, Z. Xie, K. E. deKrafft, W. Lin, *J. Am. Chem. Soc.* **2011**, *133*, 13445–13454.

[38] C. Wang, J.-L. Wang, W. Lin, *J. Am. Chem. Soc.* **2012**, *134*, 19895 – 19908.
[39] S. Pintado, S. Goberna-Ferrón, E. C. Escudero-Adán, J. R. Galán-Mascarós, *J. Am. Chem. Soc.* **2013**, *135*, 13270 – 13273.
[40] S. Wang, Y. Y. Hou, S. Lin, X. Wang, *Nanoscale* **2014**, *6*, 9930 – 9934.
[41] M.-T. Zhang, Z. Chen, P. Kang, T. J. Meyer, *J. Am. Chem. Soc.* **2013**, *135*, 2048 – 2051.
[42] D. R. Weinberg, C. J. Gagliardi, J. F. Hull, C. F. Murphy, C. A. Kent, B. C. Westlake, A. Paul, D. H. Ess, D. G. McCafferty, T. J. Meyer, *Chem. Rev.* **2012**, *112*, 4016 – 4093.
[43] C. C. L. McCrory, S. Jung, M. I. Ferrer, S. M. Chatman, J. C. Peters, T. F. Jaramillo, *J. Am. Chem. Soc.* **2015**, *137*, 4347 – 4357.
[44] CCDC 1426885 (**Co-WOC-1**) contains the supplementary crystallographic data for this paper. These data can be obtained free of charge from The Cambridge Crystallographic Data Centre.

Received: October 14, 2015
Published online: January 12, 2016

